



Valorization of tapioca stem waste: Fabrication, characterization of biochar and iron enriched biochar and scheming of DTPA iron in acidic sandy loam soil

Mathesh A^{a*}, Arivazhagan K^a, Senthilvalavan P^a, Natarajan S^b and Mathivanan N^c

^aDepartment of Soil Science and Agricultural Chemistry, Faculty of Agriculture, Annamalai University, Tamil Nadu, India

^bDepartment of Agronomy, Faculty of Agriculture, Annamalai University, Tamil Nadu, India

^cDepartment of Chemistry, Faculty of Science, Annamalai University, Tamil Nadu, India

*Corresponding author email: mathesh.agri@gmail.com

ABSTRACT

Purpose crop wastes are underused as organic resources due to low heating value and slow decomposition rates. Conversion of organic wastes into value added material like biochar through pyrolysis could offer agronomic and environmental benefits. Present study detailing about biochar synthesis from tapioca stem waste, assessing its physicochemical, morphological properties, and application of modified material to improve soil fertility and productivity. Biochar (BC) synthesized by kiln method using tapioca stalk wastes as feedstock, and enriched with ferrous sulphate into Fe enriched BC. Biochar and Iron enriched biochar (FeEBC) were characterized through XRD (X-ray diffraction), FT-IR (Fourier Transformation Infrared Spectroscopy SEM (Scanning electron microscopy) and SEM - EDS. XRD studies of synthesized BC and FeEBC proved that biochars have amorphous and non crystalline structure. The FT-IR results confirmed the presence of functional groups between 3,000 to 6000 cm⁻¹. The SEM image of BC and FeEBC confirm the presence of pores in ellipsoidal and elongated shapes. SEM - EDS characterization of BC and FeBC has been classified with, C (63.34% and 65.09%), O (24.85% and 22.02%), Mg (1.82% and 2.22%), Al(1.21% and 1.24%), K (4.89% and 4.96%), Ca(3.23% and 2.99%), Fe (0.40% and 1.01%) and S (0.22% and 0.49%) on weight basis, respectively. The elemental composition from SEM-EDS have confirmed that higher iron percentage in FeEBC than BC. BC and FeEBC were studied for their Fe release pattern through incubation experiment. Incubation results revealed that FeEBC significant DTPA extractable Fe up to the period of 120 days of incubation in acidic sandy loam soil. Also at 90 DAI (9.75 mg Kg⁻¹) and 120 DAI (9.47 mg Kg⁻¹) higher DTPA - Fe was observed with FeEBC when compared to all other treatments tested including control.

Keywords: Acid soil, Biochar, Ferrous sulphate, Iron enriched biochar, DTPA-Fe, Pyrolysis, Tapioca stem waste

Received 25.01.2023

Revised 15.02.2023

Accepted 19.03.2023

INTRODUCTION

The productivity of agricultural soil must be increased globally due to the rapid increase in global population. One of the most crucial management techniques for the sustainability of agricultural output is to increase, protect, and preserve soil fertility [44]. Besides sustainable crop production, producing nutrient-rich food is vital one in concern with malnutrition and undernourishment of human beings "as it acts as a living bridge between soil and human health" [63]. The nutritional value of a crop is determined by how it accumulates the necessary nutrients. Using various ways of fortification it can be achieved in food crops [1]. Worldwide by natural soils are formed with problems and it is aggravated by anthropogenic activities and one of its kind is acidic soils that includes cultivated and uncultivated lands [2, 3]. One-third of India's cultivated land become acidic conditions due to acidic parent materials, humid environment, heavy rainfall, and excessive drainage. Which are mostly contains silica, aluminum, and iron in high amounts, have lighter textured, low in organic content, low water holding capacity and high permeability [11]. Unbalanced use of different inorganic fertilizers by farmers to maintain or improve the productivity of agricultural soils make them unsustainable and less productive thus causes environmental and groundwater degradation [5, 6]. Further, excessive improper use of fertilizers led to accumulation of potential toxic heavy metals in soils (Nikita and Chauhan, 2020). Therefore, it is necessary to recognize a suitable soil management approach that should decrease the requirement of inorganic fertilizers that augments soil fertility and productivity. Over the past two decades, biochar usage has attracted growing

interest in sustainable agriculture [10, 4]. Bio-char's chelation properties enhancing the use efficiency of added inputs and helps to increase productivity of crop plants and also have added advantages in soil health [6, 43].

Tapioca (*Manihot esculenta Crantz*) is one of the most significant dietary energy sources, native of South America. The worldwide output of tapioca climbed from 226 million tonnes in 2007 to 292 million tonnes in 2017, according to the World Federation of Food and Agriculture Organization [44] statistics. During tapioca processing, a vast amount of trash consisting mostly of tapioca stem is wasted are often disposed of by landfilling and/or open burning, which not only consumes land resources but also pollutes the environment. Whilst transform these waste into goods with additional value a simple and eco-friendly method is required. Open burning of biomass often results in the emission of gases such as CO₂, CH₄, CO, N₂O, NH₃, SO₂, volatile organic compounds, and particulate matter into the atmosphere, which contributes to environmental changes and global warming [45]. In addition, ash, the byproduct of full combustion, includes extremely a small number of nutritional components, such as P, K, Ca, Mg, and few micronutrients. Because of this, burning cannot be considered as a significant and practical technique for handling bio wastes [46]. However, biowastes can be efficiently recycled by making into 'biochar,' a comparatively green technology management tool, via pyrolysis process in which organic material is thermally combusted in the absence of oxygen and at a relatively low temperature [47]. This technique is, in reality, the modernized form of an old pre-Columbian technique developed by Amazonian natives to enhance soil fertility [48]. It can retain carbon for extended periods of time since it is more chemically and biologically stable in soil (100-1000 years). The production of biochar and its storage in soils has been proposed as a potential method for minimizing the CO₂ concentration in the atmosphere [80]. The ability of biochar to mitigate climate change is largely attributable to its extremely resistant nature, which reduces the pace at which photo synthetically fixed carbon is returned to the atmosphere. Chemically reactive groups in biochar (such as carboxyl, hydroxyl, and ketones) assist to adsorb hazardous chemicals such as Al and Mn from acid soils, hence enabling biochar to improve degraded soils and reduce soil acidity (Lin et al., 2018). Due to the predominance of aromatic carbon, biochar becomes biochemically resistant compared to the use of raw materials as such [79]. The expanded surface area of biochar grasp greater capacity to retain water and nutrients, soil pH reduction and augmentation of CEC [14]. Biochar amended soils enhanced the nutrient availability to crop plants by augmenting the nutrient supply mechanism of soil pool significantly. Further fortified biochar as organic manure as well as amendment improves the soil quality [40].

Acid soils have many issues in nutrient availability thus affects the soil productivity. Hence, acid soils must be properly managed to make them productive using apt amendments. Amending acid soils with various sources like lime may results stabilizing the pH towards neutral but it is not sufficient to make them high productive. Where supplementing amendments like biochar plays key role in managing soil pH, improving nutrient availability via improved cation exchange capacity and adding soil organic carbon greatly. For this purpose, the present work was taken to produce biochar from tapioca stem waste. Characterization of biochar and FeEBC were under taken for ultimate analysis, XRD, SEM, SEM-EDS and FT-IR investigations. And perhaps most substantially, this research focuses on the biochar enriched with iron and evaluation of the Fe release pattern in acid soil using produce biochar and FeEBC compared with FeSO₄, and FYM .

MATERIAL AND METHODS

Preparation of Biochar and Iron enriched Biochar

Collection and processing of tapioca stalk waste

The leftover tapioca stalks were gathered from the farmers in Narippalli village in Dharmapuri district, Tamil Nadu, India is located at 12° 06' N latitude and 78° 68' with an altitude of +297 m above mean sea level. The collected stalk wastes were chopped into smaller pieces sized between 5 and 10 centimeters using country chopper. After that, the stalk wastes were left in the shade for ten days to dry.

Biochar production and processing

Equipment: The production of biochar was carried out in kiln designed and fabricated exclusively for the purpose, using cylindrical metallic drum of 90 cm height and 60 cm diameter and the capacity of 200 litre (Plate 1). An opening was provided at the top to load the inputs and also collect the final product of biochar. Air entry into the kiln was regulated by giving ten rectangular holes at the bottom. By attaching a 5 mm wire mesh at the bottom just above the base, which enables separation of biochar and ash was enabled. A vent of 115 cm height was attached at the top to exhaust the smoke [21].



**Plate 1. Biochar production by using Country Kiln
(Model adopted from ICRIDA, 2018)**



**Plate 2. Raw material
(Tapioca stem waste)**

Dried tapioca stalk wastes were fed into the inlet, and a PVC pipe was placed in the centre of the kiln to provide a central vent. After the drum had reached capacity, the pipe was taken out. The biomass was burned by smearing a little amount of fuel on tapioca stems. As demonstrated by the thinning of the smoke, seal the intake to limit the flow of air, so decreasing the likelihood that the stalk will be turned to ash. When the flame turned blue, plug all of the openings in the kiln with mud to keep the smoke contained entirely inside the drum. Initially, the time required for biochar production was fixed. After 2-2.5 hours, the kiln was permitted to cool and 'biochar' was collected (CRIDA -NICRA research bulletin, 2018). Using an infrared thermometer, the pyrolysis temperature was determined to range between 350 and 400°C during the process. A known quantity of tapioca stem waste undergone pyrolysis and weight of biochar obtained was recorded. Nearly 15 Kg of tapioca stalk waste was filled in drum kiln at a time and at the end of the pyrolysis process it yields 4 to 4.5 Kg of biochar. Recovery of biochar was calculated and found to be 25-30 per cent. The biochar was crushed initially by tractor (plate 3&4) and using wooden mallet. At last, the powdered biochar is sieved through 2mm sieve for further use.



Plate 3. Crushing of biochar by tractor



Plate 4. Crushed tapioca stem waste biochar (TSWBC)

Preparation of Fe enriched biochar (FeEBC) using FeSO_4

Fe enriched biochar was produced by mixing 250 kg of tapioca stems waste biochar (TSWBC) with 1.25 kg of ferrous sulphate. It was planned towards evaluation of biochar, and Fe enriched biochar to fortify iron availability in acidic soil. Layer of biochar was laid at the base of the heap, and allowing the ferrous sulphate solution to adhere readily as it was sprinkled gently on top using sprayer for even distribution. Then a second layer of biochar was applied on top of the first layer, followed by the addition of ferrous sulphate solution. Similarly, the third and fourth layers followed the same procedure. The top section of the material was blended manually. The bed was sprinkled with water to keep wet. The biochar and ferrous sulphate were then properly mixed by 2-3 turns. At each rotation, the whole material is fully mixed. Further, the heaped biochar and iron sulphate mixture was filled in a pit and it was plastered with a 2-3 cm layer of mud and cattle dung mixture (plate 4). The materials are allowed to remain without turning and watering for 45 days. After completion of incubation period the mixture of iron enriched biochar collected, shade dried sieved and stored (plate 5 and 6) and involved for different physico-chemical properties and morphological characterization analysis.



Plate 5. Incubating Fe enriched biochar (mudding process during incubation)



Plate 6. Sieving of biochar



Plate 6. Final product iron enriched biochar (FeEBC)

Characterization of biochar

Physically, biochar has a low bulk density owing to its porous structure, which results in a high specific surface area ranging from 50 to 900 $\text{m}^2 \text{g}^{-1}$ and a high water-holding capacity [24, 6]. From a chemical standpoint, the most notable characteristic of biochar is its polycondensations aromatic structure [56], which is the result of dehydration during thermo-chemical conversion [57] and it is responsible for dark colour. This structure also accounts for its greater resistance relative to all other organic materials in the environment. Furthermore, compartments of basic ash result in a high pH value.

Recent studies have showed that the feedstock quality and production circumstances, such as pyrolysis temperature and residence time, have a substantial effect on the amount, quality, and elemental compositions of biochar [58, 59, 60]. Consequently, the selection of acceptable feedstock and the

appropriate pyrolysis technique are critical for biochar manufacturers in order to produce a biochar amendment that is tailored to solve a particular agricultural soil problem. The amount of volatile matter in low temperature biochar is high, but the amount of fixed carbon (FC) and ash is lower than in high temperature biochar [61]. Total C, fixed carbon (FC), and ash content of biochar are more reliant to feedstock than pyrolysis temperature, although volatile matter and biochar output are temperature-dependent [62]. Following the methodology proposed by Rajkovich et al., [55] the pH and EC of biochar were determined by using a modified dilution of 1:10 (biochar: deionized water) it was agitated and equilibrated with deionized water for one hour. The structural and surface analyses were also investigated with the help of Fourier Transformed Infrared spectroscopy (FT-IR), Scanning Electron Microscopy (SEM), Energy Dispersive X-ray Spectroscopy (EDS), and X-ray diffraction spectroscopy (XRD) tests were carried out at Department of Physics, Faculty of Science, Annamalai University, and Tamil Nadu.

Determination iron release pattern

Incubation experiment

An incubation experiment was carried out to investigate the Fe release pattern of biochar, FeEBC, FYM, FeEFYM and FeSO₄ in acidic sandy clay loam soil in the PhD laboratory, Department of Soil Science and Agricultural Chemistry. Surface soil sample was taken from a farmers holding in the Narippalli hamlet of the Harur block in Dharmapuri District, Tamil Nadu, and India. The findings of soil properties are presented in table 1. The soil was air-dried and sieved through 2 mm mesh screen. The treatments were applied as per treatment schedule planned. Gravimetric water content of the soil was brought up to the field capacity level by adding measured quantity of distilled water. The treatments used are as follows, Absolute control (T1), FeSO₄ (T2), Biochar (T3), Iron Enriched Biochar (T4), Farm Yard Manure (T5), and Iron Enriched Farm Yard Manure (T6). The study material was used in accordance with the amount of Fe present in the various iron sources. In particular, the amount of iron contained in ferrous sulphate @ Fe 25 kg ha⁻¹ equivalent iron enhanced biochar (548 kg ha⁻¹) and FYM (521 kg ha⁻¹) were applied. The experiment was carried out in a completely Randomized Design, replicated four times. The outcomes of investigations into the physico-chemical characteristics of biochar and iron enriched biochar are presented in table 1.

Table 1. Physico-chemical properties of experimental soil, Biochar and iron enriched biochar

Properties		Content values of		
		Experimental Soil	Tapioca Stem Waste Biochar (TSWBC)	Iron enriched biochar (FeEBC)
Mechanical	Fine Sand (%)	36.07	-	-
	Coarse Sand (%)	28.0	-	-
	Silt (%)	16.43	-	-
	Clay (%)	19.08	-	-
	Soil textural class	Sandy loam	-	-
	Taxonomic class	Fluventic Haplustalf	-	-
Physical	Bulk density (Mg m ⁻³)	1.53	0.35	0.34
	Particle density (Mg m ⁻³)	2.22	0.82	0.85
	Total porosity (%)	31.08	57.31	60.0
	Available moisture content (%)	1.37	1.40	1.41
	Recovery (%)	-	30.25	30.25
	Ash (w w ⁻¹)	-	1.25	1.25
Chemical properties	pH (1:2:5) / (1:20)	4.86	9.18	9.06
	EC (dS m ⁻¹) / (1:10)	0.08	1.44	1.42
	CEC [cmol (p) Kg ⁻¹]	3.55	15.69	14.98
	Organic Carbon (g kg ⁻¹)	25	737.6	738.1
	Available N (kg ha ⁻¹) / Total N (g kg ⁻¹)	182	1.11	1.13
	Available P (kg ha ⁻¹) / Total P (g kg ⁻¹)	36.50	1.18	1.19
	Available K (kg ha ⁻¹) / Total K (g kg ⁻¹)	100.7	14.96	14.96
	Available S (mg kg ⁻¹) / Total S (mg kg ⁻¹)	7.49	4.92	7.58
Available Fe (mg kg ⁻¹) / Total Fe (mg kg ⁻¹)	3.37	8660	3760	

Application of iron sources

For this incubation investigation, it was intended to fill each pot with 200 g of soil. At first, 190 g of soil was weighed and placed in each container. Subsequently, for this incubation study, each treatment will be replicated four times, and five soil samples will be collected at intervals. A total of 20 pots will be used for each treatment. The estimated amounts of BC, FeEBC, FYM, and FeEFYM are added to 200g of soil and well mixed in preparation for the evenly spread of iron sources in soil. 10g of the soil and Fe source blend was weighed and transferred to a designated container, followed by a thorough mixing of the soil with the various iron sources. The application of ferrous sulphate to 20 containers was estimated according to the treatment schedule. In order to make a solution, 200 ml of distilled water was added to the calculated FeSO_4 . Thereafter, 10 ml of aqueous aliquots of FeSO_4 solution were pipetted and placed to the treatment-appropriate pots. Table 3 displays the iron content and amendment application per hectare for various iron sources utilized in the incubation experiment analyzed in AAS as per the standard procedure. The soil was incubated at field capacity for four months (120 days), with distilled water supplied every two days to maintain constant moisture content during the incubation period. After incubation, samples were taken at certain intervals, viz 0, 30, 60, 90, and 120 days, and assessed for iron release pattern. DTPA technique was applied to analyze DTPA-extractable iron [62-67]

Table 2. Different iron sources used for incubation study for determining Fe release in acidic pH soil

Sources	Iron content (%)	Sources applied based on iron content	
		Kg ha ⁻¹	g pot ⁻¹ (200 g of soil)
Ferrous sulphate ($\text{FeSO}_4 \cdot 7\text{H}_2\text{O}$)	19	25	0.0025
Biochar alone (TSWBC)	0.37	1263	0.126
Iron enriched biochar (FeEBC)	0.87	548.49	0.054
Farm yard manure (FYM)	0.49	975.35	0.097
Iron enriched Farm yard manure (FeEFYM)	0.91	520.83	0.052

Statistical analysis

Each dataset was summarized through calculating average and standard deviation. The data collected were statistically analyzed using SPSS statistical package version 11.0. One-way analysis of variance (ANOVA) was used to test the differences between control and other treatments. The interpretation of treatment effects was made on the basis of critical difference at (P=0.05) probability level. The Duncan's multiple range tests was used to segregate the significance of difference among the mean values obtained for observed parameters.

RESULTS AND DISCUSSION

Characterization of Tapioca stem waste biochar (TSWBC) and iron enriched biochar (FeEBC) SEM (Scanning Electron Microscopy) with EDS

Using SEM and SEM-EDS micrographs, the surface morphology of tapioca stem waste biochar (TSWBC) was investigated. The SEM (Fig. 1a) and SEM-EDS (Fig. 1b) micrographs illustrate the various magnifications of synthesized TSWBC. The TSWBC picture showed dispersed pores of tiny size, a circular, ellipsoidal, and elongated structure, and a compartmental, rectangular pattern of varying size. The SEM EDS analysis of tapioca stalk waste BC revealed the following elemental compositions on a weight basis: C (63.34%), O (24.85%), Mg (1.82%), Al(1.21%), K (4.89%), Ca(3.23%), Fe (0.40%), and S (0.22%).

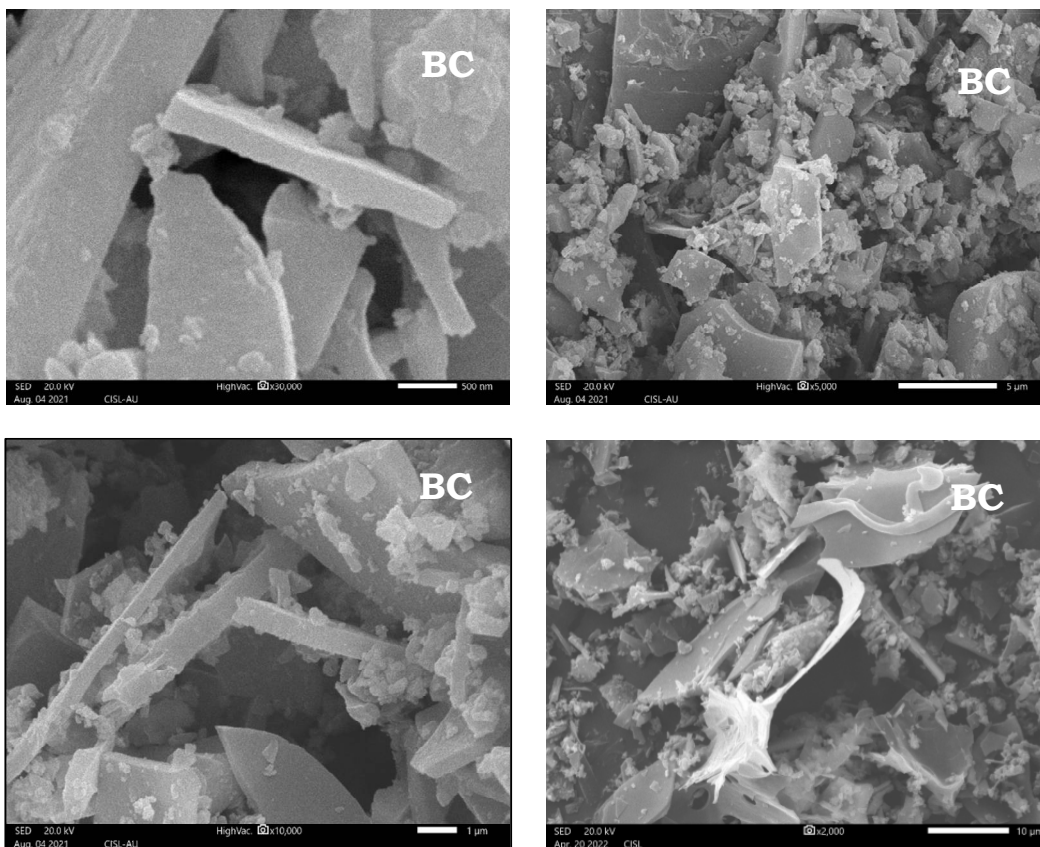
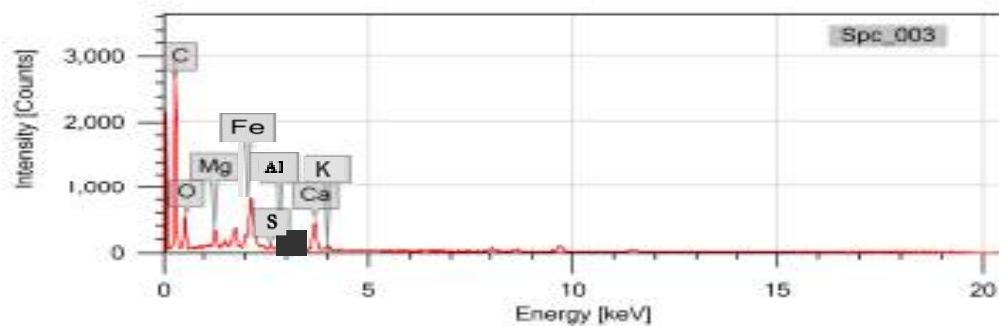
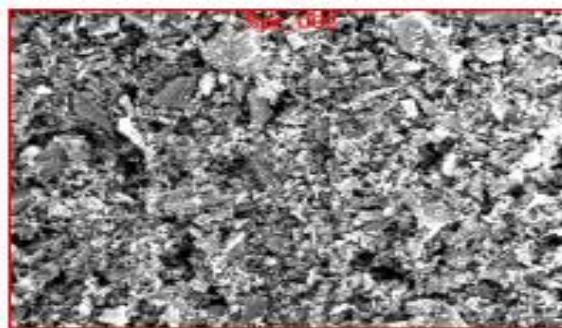


Fig. 1a. SEM image for tapioca stem waste biochar (TSWBC)



Element Line		Mass%	Atom%
C	K	63.34±0.29	72.95±0.34
O	K	24.85±0.36	22.59±0.30
Mg	K	1.82±0.05	0.93±0.03
Al	K	1.21±0.04	0.61±0.02
K	K	4.89±0.04	1.68±0.01
Ca	K	3.23±0.07	1.09±0.02
Fe	K	0.40±0.04	0.10±0.01
S	K	0.22±0.10	0.05±0.01
Total		100.00	100.00
SpC_002		Fitting ratio 0.3947	

Fig. 1b SEM-EDS image for TSW biochar

By using SEM and SEM-EDS micrographs, we were able to analyse the surface morphology of iron-enriched biochar prepared in this study [61-64]. The varied levels of magnification can be seen in the scanning electron micrographs (Fig. 1c) and scanning electron micrographs with energy dispersive spectroscopy (Fig. 1d). The image of the FeEBC looked to be of a lesser magnitude. Pores were seen to be distributed, and the structure was found to be round, ellipsoidal, and elongated [64-68]. Compartmental rectangular patterns of varying sizes were also seen. The iron-enriched biochar was analyzed by scanning electron microscopy and energy dispersive spectroscopy (SEM EDS), which indicated the elemental compositions on a weight basis as follows: C (65.09%), O (22.02%), Mg (2.22%), Al(1.24%), K (4.96%), Ca(2.99%), and S (0.49%). When compared to BC on its own, the FeEBC had a much greater amount of both iron and sulphur.

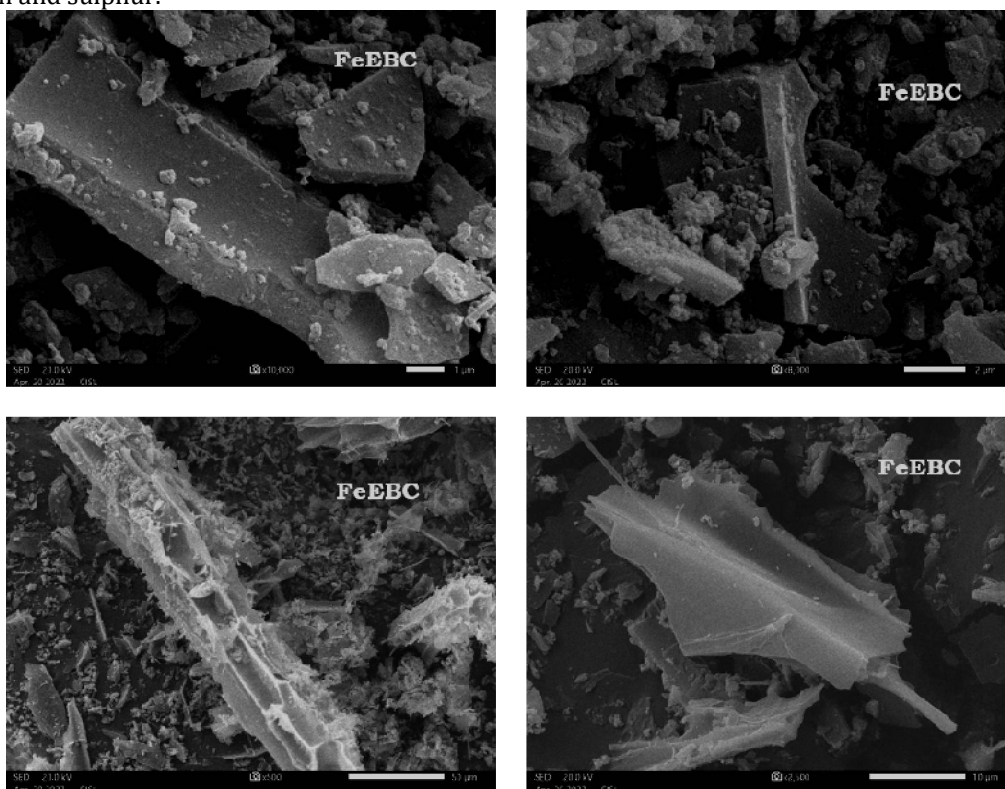
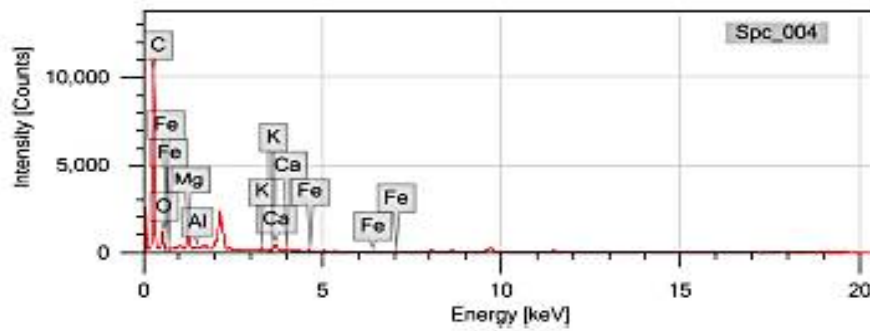
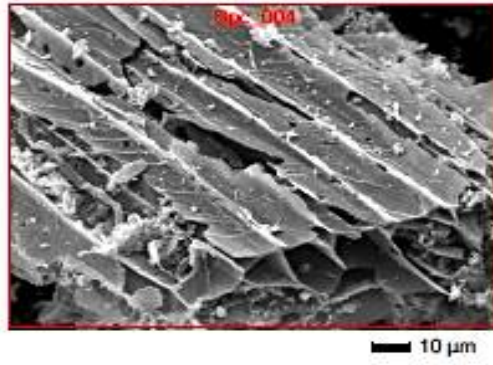


Fig. 1c SEM image for Fe enriched biochar



Element	Line	Mass%	Atom%
C	K	65.09±0.20	73.49±0.23
O	K	22.02±0.53	20.98±0.46
Mg	K	2.22±0.09	1.26±0.05
Al	K	1.24±0.31	0.75±0.15
K	K	4.96±0.27	1.80±0.05
Ca	K	2.99±0.15	1.02±0.09
Fe	K	1.01±0.04	0.56±0.01
S	K	0.49±0.04	0.09±0.02
Total		100.00	100.00
Spc_003		Fitting ratio 0.4894	

Fig. 1d SEM-EDS image for Fe enriched biochar

XRD (X-ray diffraction Spectroscopy)

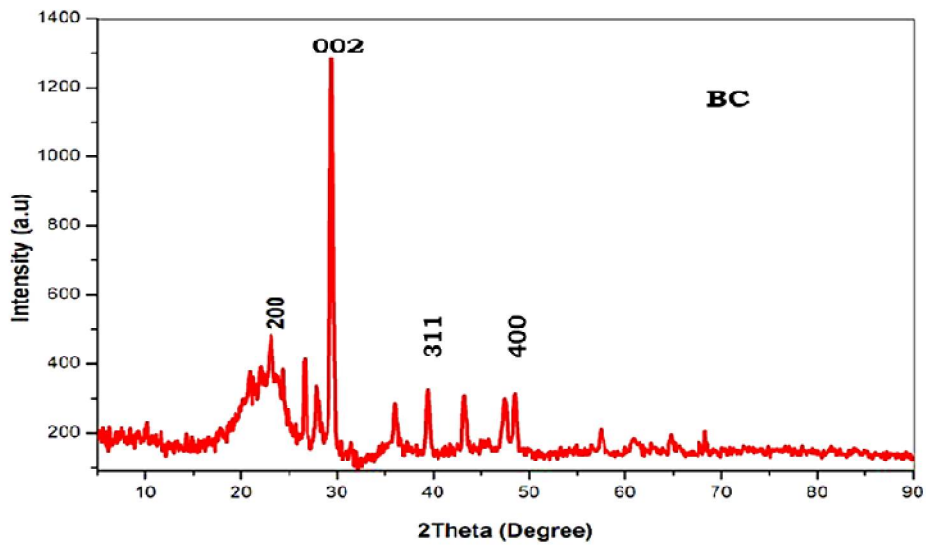


Fig. 2a XRD image for biochar

The diffractograms produced for each of the biochar considered in this investigation are shown in (Fig. 2a). This study has been used to establish that biochar is amorphous in nature. The XRD patterns reveal comparable materials, as is to be anticipated, and they point to a long-range amorphous material. The graphitic basal plan in biochar has a major wide peak that is indexed as (002). 2θ values of 24, 29, 43 and 57 corresponding to the plans of 002, 311, 100, and 101 respectively. The values are well matched with JCPDS Card No.83-1764.

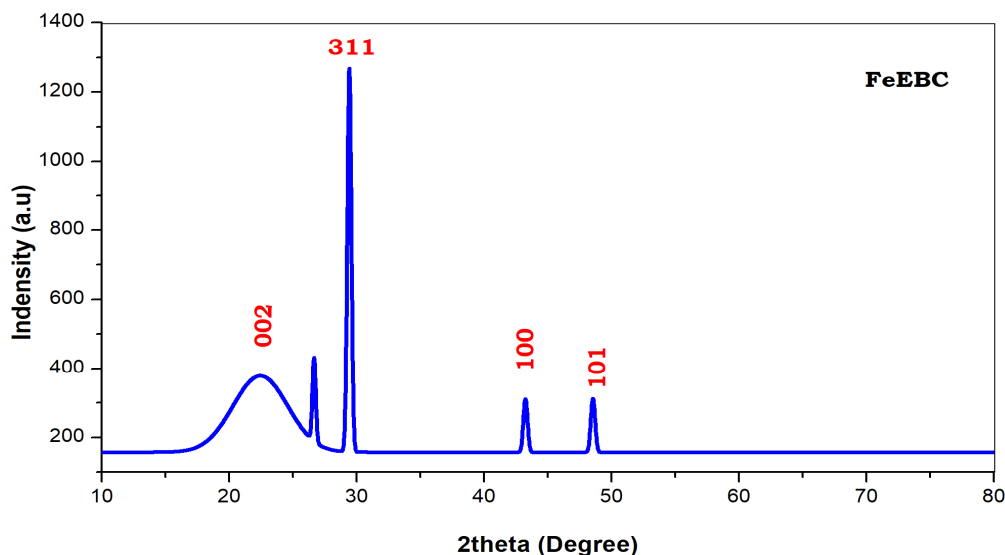


Fig. 2b XRD image for Fe enriched biochar

The diffraction peaks in the XRD spectra for the Fe-biochar preparations are faint, as illustrated in (Fig. 2b). The distinctive peaks of the FeEBC (23, 30, 44 and 48) is attributed to the plane of (002,311, 100 and 101) its well matched with JCPDS Card number (JCPDS No. 26-1136) [9]. These findings show that biochar affects mechanical performance as well as pozzolanic reactions since this sort of phase allows for stability and durability. Despite the absence of crystalline phases in the sample, it contained a high number of atoms that favoured a high number of electrons in the unit under investigation, which may have contributed to this effect [10]. However, as was already indicated, TSWBC and Fe enriched biochar are entirely amorphous, which poses no challenges for the studies since they lack any crystalline phases that would interfere with their reaction against acidic condition [67, 68].

FT-IR (Fourier Transformed Infrared Spectroscopy)

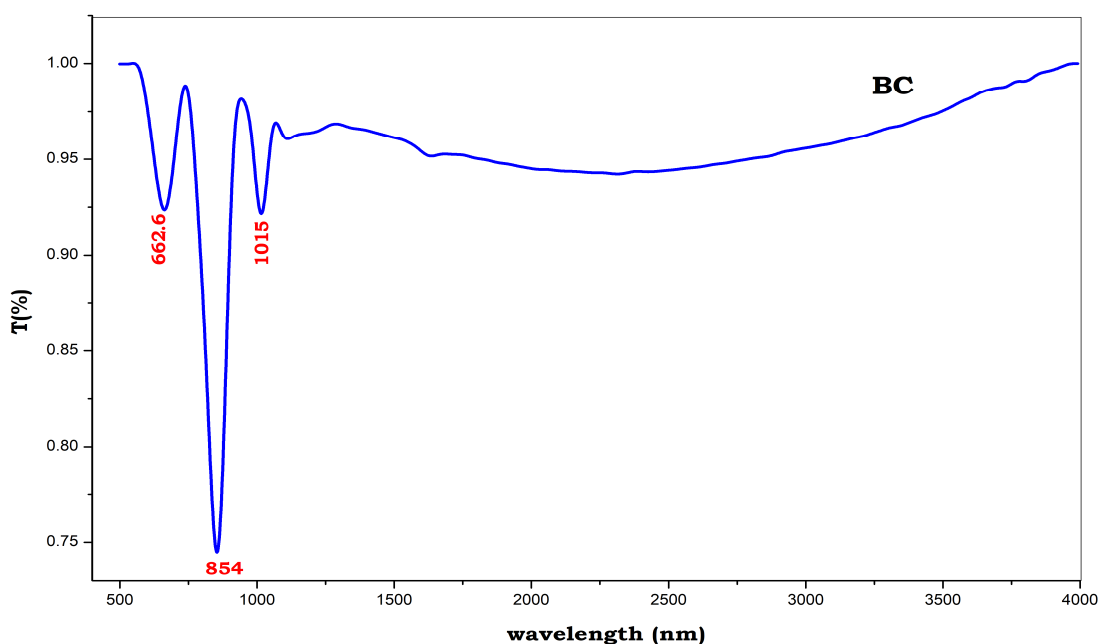


Fig. 3a FTIR image for biochar

The surface functional groups of biochar have a significant role in the adsorption of heavy metals. (Fig. 3a) depicts the FT-IR spectra of BC, which were used to determine the surface functional groups

identified by FT-IR spectroscopy. The shoulder in the vicinity of 1015 cm^{-1} corresponds to the C=O, C=C stretching vibration [16]. Attributed the peaks at 1167 cm^{-1} and 1564 cm^{-1} to the C=O stretching vibration in CO_3^{2-} and the C-O stretching vibration, respectively. The peak at 662 and 854 cm^{-1} was attributable to the aromatic C-H bonding vibration [28].

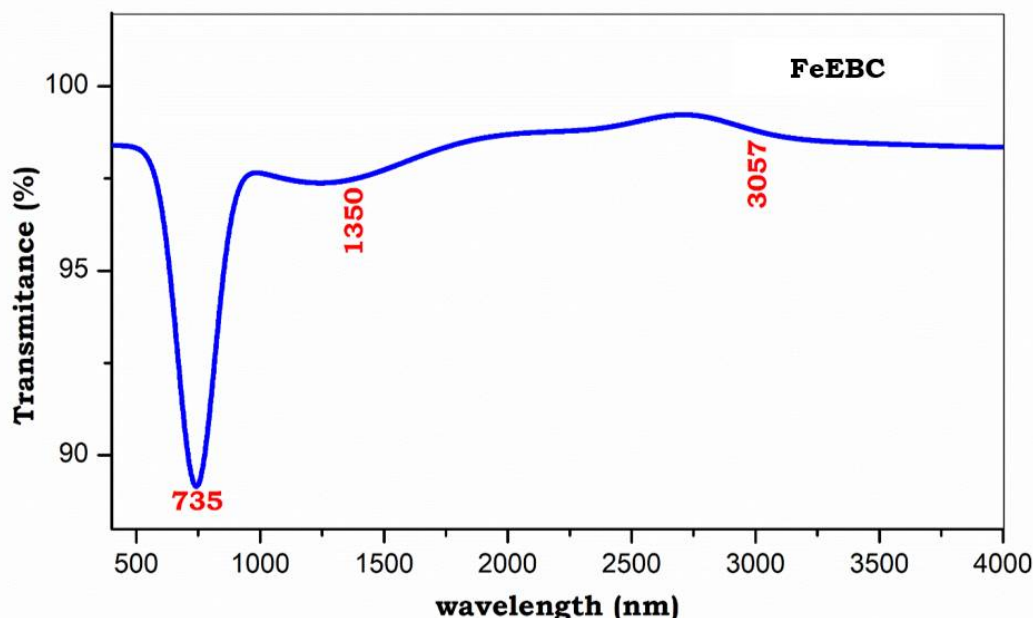


Fig. 3b FTIR image for Fe enriched biochar

Biochar surface functional groups play an important role in the adsorption of heavy metals and essential nutrient. As seen in (Fig. 3b) the surface functional groups discovered by FT-IR spectroscopy are depicted for iron enriched biochar. The C=O, C=C stretching vibration is felt in the shoulder about 1350 cm^{-1} [29-32]. C=O stretching vibration in CO_3^{2-} . The aromatic C-H bonding vibration was responsible for the peaks at 735 cm^{-1} . It showed strong intensity of hydroxyl group presenting in enriched biochar [72-76].

Iron Release Pattern (IRP) study in acidic soil

Study results showed that, application of different iron sources of iron enriched organic sources, without iron enriched organic sources and ferrous sulphate, there is a significant net changes in DTPA extractable iron in Alfisol soil is presented in table 3 [30, 35, 36]. Ferrous sulphate alone (T_2) applied soil recorded significantly higher iron release of 19.69 mg Kg^{-1} , 14.97 mg Kg^{-1} and 11.38 mg Kg^{-1} at 0, 30 and 60 DAI, respectively. Even though, DTPA extractable iron of ferrous sulphate shows the decreasing trend especially when compared to iron enriched biochar (T_4) and FYM (T_6) at all the days after incubation [33-36]. At 90 and 120 DAI the application of ferrous sulphate micro nutrient treated soil showed drastically lower (8.87 mg Kg^{-1} and 7.03 mg Kg^{-1}) DTPA extractable iron which was on par with Fe enriched with FYM and recorded higher DTPA Fe content when compared with Biochar without enriched with iron and FYM and absolute control, except Fe enriched with biochar.

Table 3. DTPA extractable iron (mg Kg^{-1}) from different sources

Treatments	Days of incubation				
	0 th DOI	30 th DAI	60 th DAI	90 th DAI	120 th DAI
Control	3.40 ^f	3.11 ^f	2.35 ^e	1.73 ^e	1.51 ^f
FeSO ₄	19.69 ^a	14.97 ^a	11.38 ^a	8.87 ^b	7.03 ^c
BC	6.59 ^e	6.08 ^e	5.92 ^d	5.04 ^c	4.53 ^d
FeEBC	11.58 ^c	11.07 ^c	10.43 ^b	9.75 ^a	9.47 ^a
FYM	7.86 ^d	6.98 ^d	5.79 ^d	4.45 ^d	4.15 ^e
FeEFYM	12.30 ^b	11.63 ^b	9.44 ^c	8.80 ^b	8.22 ^b
S.Ed	0.23	0.18	0.20	0.15	0.14
CD (p=0.05)	0.48	0.37	0.42	0.31	0.28
CV %	3.20	2.79	3.75	3.28	3.31

[DOI- Days of incubation ; C - Control, FeSO₄ - Ferrous sulphate; BC - Biochar; FeEBC - Iron enriched biochar ; FYM - Farmyard manure; FeEFYM - Iron enriched farmyard manure ; DAI - Days after Incubation ; CV-Coefficient of variation; Mean (\pm standard deviation, n =3) with the same letters are not significantly different at p < 0.05; p values were determined by ANOVA]

Initially at 0, 30 and 60 DAI the iron enriched with biochar (T₄) treated soils recorded iron release or availability was lower (11.58 mg Kg⁻¹, 11.07 mg Kg⁻¹ and 10.43 mg Kg⁻¹) but not markedly decrease in iron availability in soil when brought into comparison with all other treatments. The Fe enriched with biochar (T₄) treated soil recorded substantially higher (9.75 mg Kg⁻¹ and 9.47 mg Kg⁻¹) DTPA extractable iron at 90 and 120 days of incubation when compared to all the other treatments [48, 49]. The second highest DTPA extractable iron (8.22 mg Kg⁻¹) was recorded by iron enriched with FYM (T₆) at 120 DAI at 90 DAI the iron availability of Fe enriched FYM (8.80 mg Kg⁻¹) was close with Ferrous sulphate applied treatment (T₂). Further Biochar and FYM without iron enriched organic sources shows sustained iron release pattern at all the days after incubation when compared to ferrous sulphate and absolute control treatment they were not reach sustainability or continuous supply of Fe like Bc and FeEBC [47-50]. The biochar application to acidic soil also shows a controversial effect in micronutrient availability. A congruous result was reported by Akanji et al., [10]; Demirkaya et al., [17]. They applied the biochar obtained from poultry manure to the calcareous sandy soil in an acidified and non-acidified form. At the end of the incubation period (30 days), the increasing of the iron content was observed from acidified biochar treated soil for calcareous soil [10] and the result are vice versa for acidic soil. Most of the literatures on the effect of biochar addition on different soil improved iron availability was observed and supported this present investigation.

It is clear that iron enriched with biochar (T₄) was observed the most effective iron source in maintain the highest amount of extractable iron up to 120 days of incubation in acidic soil. Particularly after 60 DAI, DTPA extractable iron availability has been increased greatly by the application of Fe enriched with biochar. According to Demirkaya et al [17] the iron availability in soil is mostly pH dependent and also the organic matter content in the soil. The application of iron biochar enriched biochar might have propelled the Fe supply due to pores presence with higher surface area, cation exchange capacity and modulated the release of said element. In addition to, the biochar sources are mostly higher pH in alkaline condition. Therefore, the enriched biochar combined with soil, equilibrate the soil pH, which aids to made more iron availability acidic conditions.

The mechanism behind the iron release may be that functional groups present in the biochar get participated in adsorption and complexation of iron impregnated. When organic carbon content increased in the soil through biochar addition may stimulate the hydroxyl and carboxyl groups when hydrated. Consequently iron adsorbed and complexed on the surface of biochar might have undergone dissolution to increase iron mobility and availability in soil by increased cation exchange.

CONCLUSIONS

Tapioca stem waste biochar produced by country kiln method adopted from CRIDA and iron enriched biochar was prepared by mixing biochar with ferrous sulphate at the ratio of 200:1(w/w basis). Characterization of biochar and iron enriched biochar by SEM and SEM-EDS revealed that surface morphology and presence of various elements (C, O, Mg, Al, K, Ca, Fe & S), XRD analysis proved amorphous structures of BC and FeEBC, and FTIR analysis confirmed the presence functional groups (C=O, C=C, C-H) on BC and FeEBC. So, microstructural analysis reveals a porous biochar structure being surrounded by layers of mineral, organo-complexes. From the incubation study results, DTPA extractable iron in soil was significantly increased by all the sources tested compared to control. Particularly, application of iron-enriched biochar was more effective than all other sources used. Iron enriched biochar (FeEBC) application showed higher iron availability and sustainable nutrient release in acidic pH soil. The findings of the study can bring lights on iron fortification in food crops via waste based biochar from tapioca stem waste and pave a new path of iron fortification in acidic soil pH conditions where iron present more in soil pool but not to plants.

REFERENCES

1. Agegnehu G, Amede T, Erkossa T, Yirga C, Henry C, Tyler R, Nosworthy M.G, Beyene S, Sileshi G.W., (2021). Extent and management of acid soils for sustainable crop production system in the tropical agroecosystems: a review. *Acta Agriculturae Scandinavica, Section B- Soil & Plant Science* 71(9):852-869.
2. Ahamed, M., Karns, M., Goodson, M., Rowe, J., Hussain, S.M., Schlager, J.J., Hong, Y.L., (2008). DNA damage response to different surface chemistry of silver nanoparticles in mammalian cells. *Toxicol. Appl. Pharmacol.* 233 (3), 404-410.
3. Ananth, A.N., Daniel, S.C.G.K., Sironmani, T.A., Umaphathi, S., (2011). PVA and BSA stabilized silver nanoparticles based surface-enhanced plasmon resonance probes for protein detection. *Colloids Surf. B* 85 (2), 138-144.
4. Anderson, D.S., Silva, R.M., Lee, D., Edwards, P.C., Sharmah, A., Guo, T., Pinkerton, K.E., Van Winkle, L.S., (2015). Persistence of silver nanoparticles in the rat lung: influence of dose, size, and chemical composition. *Nanotoxicology* 9 (5), 591-602.

5. Anker, J.N., Hall, W.P., Lyandres, O., Shah, N.C., Zhao, J., Van Duyne, R.P., (2008). Biosensing with plasmonic nanosensors. *Nat. Mater.* 7 (6), 442–453.
6. Antsiferova, A., Buzulukov, Y., Demin, V., Kashkarov, P., Kovalchuk, M., Petrinskaya, E., (2015). Extremely low level of Ag nanoparticle excretion from mice brain in in vivo experiments. *IOP Conf. Ser. Mater. Sci.* 98, 1–6.
7. Arora, S., Jain, J., Rajwade, J.M., Paknikar, K.M., 2009. Interactions of silver nanoparticles with primary mouse fibroblasts and liver cells. *Toxicol. Appl. Pharmacol.* 236 (3), 310–318.
8. AshaRani, P.V., Mun, G.L.K., Hande, M.P., Valiyaveetil, S., 2009. Cytotoxicity and genotoxicity of silver nanoparticles in human cells. *ACS Nano* 3 (2), 279–290.
9. Austin, C.A., Umbreit, T.H., Brown, K.M., Barber, D.S., Dair, B.J., Francke-Carroll, S., Feswick, A., Saint-Louis, M.A., Hikawa, H., Siebein, K.N., Goering, P.L., 2012. Distribution of silver nanoparticles in pregnant mice and developing embryos. *Nanotoxicology* 6 (8), 912–922.
10. Akanji MA, Usman ARA, Al-Wabel M.I., 2021. Influence of acidified biochar on CO₂-C efflux and micronutrient availability in asandy soil. *Sustainability* 13: 5196.
11. Allen L, De Benoist B, Dary O, Hurrell R (2006). Guidelines on food fortification with micronutrients. World Health Organization and Food and Agriculture Organization of the United Nations; Accessed September 20, 2022.
12. Awad Y.M, Lee S.S, Kim K.H, Ok Y.S, Kuzyakov Y., (2018). Carbon and nitrogen mineralization and enzyme activities in soil aggregate-size classes: Effects of biochar, oyster shells, and polymers. *Chemosphere* 198: 40–48.
13. Bray R.H, Kurtz L.T., 1945. Determination of total, organic, and available forms of phosphorus in soils. *Soil Sci* 59: 39–46.
14. Bagheri-Abassi, F., Elder, A., Gelein, R., Silva, V., Feikert, T., Opanashuk, L., Carter, J., Potter, R., Maynard, A., Ito, Y., Finkelstein, J., Oberdorster, G., (2006). Translocation of inhaled ultrafine manganese oxide particles to the central nervous system. *Environ. Health Perspect.* 114 (8), 1172–1178.
15. Cheng C, Lehmann J, Thies J.E, Burton S.D, Engelhard M.H., (2006). Oxidation of black carbon by biotic and abiotic processes. *Org. Geochem* 37: 1477–1488.
16. CRIDA, (2018). Biochar production and its use in rain fed agriculture: Experiences from CRIDA. CRIDA-NICRA Research Bulletin 2018, ICAR - Central Research Institute for Dry land Agriculture, Hyderabad. pp50.
17. Demirkaya S, Gulser C, Ay A., (2021). The effect of iron enriched acidified and non-acidified biochars on DTPA extractable iron content of a calcareous soil. Symposium: Soil Science and plant Nutrition.
18. El-Naggar A.H, Usman A.R, Al-Omran A, Ok Y.S, Ahmad M, Al-Wabel M.I., 2015. Carbon mineralization and nutrient availability in calcareous sandy soils amended with woody waste biochar. *Chemosphere* 138: 67–73.
19. Food and Agriculture Organization (FAO) Production crop data, 2017.
20. Fong, J., Wood, F., (2006). Nanocrystalline silver dressings in wound management: a review. *Int. J. Nanomedicine* 1 (4), 441–449.
21. Hadroug S, Jellali S, Azzaza A, Kwapinska M, Hamdi H, Leahy J, Jegurium M, Kwapinski W., (2022). Valorization of salt post-modified poultry manure biochars for phosphorus recovery from aqueous solutions: investigations on adsorption properties and involved mechanism. *Biomass Conversion and Biorefinery* 12:4333–4348.
22. Jackson ML, (1973). Soil Chemical analysis. Prentice Hall of India (Pvt.) Ltd., New Delhi.
23. Krasnikov P, Tobaoda M.A, Amanullah., (2022). Fertilizer use, soil health and agricultural sustainability. *Agriculture* 12:462.
24. Lehmann, J, (2007). A handful of carbon. *Nature* 447: 143–144.
25. Lin Q, Zhang L, Rianza M, Zhang M, Xia H, Lv B, Jiang C., (2018). Assessing the potential of biochar and aged biochar to alleviate aluminum toxicity in an acid soil for achieving cabbage productivity. *Ecotoxicol. Environ. Safety* 161: 290–295.
26. Lindsay WL, Norvell W.A., (1978). Development of a DTPA micronutrient soil test for zinc, iron, manganese, and copper. *Soil Sci. Soc. Am. J* 42:421–428.
27. Lankveld, D.P.K., Oomen, A.G., Krystek, P., Neigh, A., Troost-de Jong, A., Noorlander, C.W., Van Eijkeren, J.C.H., Geertsma, R.E., De Jong, W.H., (2010). The kinetics of the tissue distribution of silver nanoparticles of different sizes. *Biomaterials* 31 (32), 8350–8361.
28. Lansdown, A.B., (2010). A pharmacological and toxicological profile of silver as an antimicrobial agent in medical devices. *Adv. Pharmacol. Sci.* 2010, 910686.
29. Lee, J.H., Kim, Y.S., Song, K.S., Ryu, H.R., Sung, J.H., Park, J.D., Park, H.M., Song, N.W., Shin, B.S., Marshak, D., Ahn, K., Lee, J.E., Yu, I.J., (2013). Biopersistence of silver nanoparticles in tissues from Sprague-Dawley rats. *Part. Fibre Toxicol.* 10 (36), 1–14.
30. Lem, K.W., Choudhury, A., Lakhani, A.A., Kuyate, P., Haw, J.R., Lee, D.S., Iqbal, Z., Brumlik, C.J., (2012). Use of nanosilver in consumer products. *Recent Patents Nanotechnol.* 6 (1), 60–72.
31. Levard, C., Reinsch, B.C., Michel, F.M., Oumahi, C., Lowry, G.V., Brown, G.E., (2011). Sulfidation processes of PVP-coated silver nanoparticles in aqueous solution: impact on dissolution rate. *Environ. Sci. Technol.* 45 (12), 5260–5266.
32. Limbach, L.K., Wick, P., Manser, P., Grass, R.N., Bruinink, A., Stark, W.J., (2007). Exposure of engineered nanoparticles to human lung epithelial cells: influence of chemical composition and catalytic activity on oxidative stress. *Environ. Sci. Technol.* 41 (11), 4158–4163.
33. Liu, J.Y., Hurt, R.H., (2010). Ion release kinetics and particle persistence in aqueous nano-silver colloids. *Environ. Sci. Technol.* 44 (6), 2169–2175.
34. Liu, W., Wu, Y., Wang, C., Li, H.C., Wang, T., Liao, C.Y., Cui, L., Zhou, Q.F., Yan, B., Jiang, G.B., (2010). Impact of silver nanoparticles on human cells: effect of particle size. *Nanotoxicology* 4 (3), 319–330.

35. Liu, F., Chung, S., Oh, G., Seo, T.S., (2012a). Three-dimensional graphene oxide nanostructure for fast and efficient water-soluble dye removal. *ACS Appl. Mater. Interfaces* 4 (2), 922–927.
36. Liu, G.P., Jin, W.Q., Xu, N.P., (2015). Graphene-based membranes. *Chem. Soc. Rev.* 44 (15), 5016–5030.
37. Liu, L., Li, C., Bao, C.L., Jia, Q., Xiao, P.F., Liu, X.T., Zhang, Q.P., 2012b. Preparation and characterization of chitosan/graphene oxide composites for the adsorption of Au(III) and Pd(II). *Talanta* 93, 350–357.
38. Liu, L., Liu, S.X., Zhang, Q.P., Li, C., Bao, C.L., Liu, X.T., Xiao, P.F., (2013). Adsorption of Au(III), Pd(II), and Pt(IV) from aqueous solution onto graphene oxide. *J. Chem. Eng. Data* 58 (2), 209–216.
39. Mansuri S.A, Shakhela R.R, Kashyapkumar N.P, JatJ,S., (2019). Effect of different zinc enriched organics on nutrient content and uptake by summer pearl millet (*Pennisetum glaucum* L.) on loamy sand. *Journal of Pharmacognosy and Phytochemistry* 8(1): 724-730.
40. Martinsen V, MulderJ, Shitumbanuma V, SparrrevikM, BorresenT, Cornelissen G., (2014). Farmer-led maize biochar trials: Effect on crop yield and soil nutrients under conservation farming. *Journal of Plant Nutrition and Soil Science* 175: 698-707.
41. Mehmood K,Wu Y, Wang L, Yu S,LiP,ChenX,LiC,ZhangY,LiM,LiuW,WangY,Liu Z,ZhuY,RosenfeldD,SeinfeldJ.H., (2020). Relative effects of peon biomass burning and open crop straw burning on haze formation over central and eastern China: modeling study driven by constrained emissions. *Atmos.Chem.Phys* 20:2419-2443.
42. Naeem MA, Khalid M, Aon M, Abbas G, Tahir M, Amjad M, Murtaza B, Yang A, Akhtar S.S.,2014. Effect of wheat and rice straw biochar produced at different temperatures on maize growth and nutrient dynamics of a calcareous soil. *Archives of Agronomy and Soil Science* 63: 2048-2061.
43. Nikita B,ChauhanP.S.,(2020). Excessive and disproportionate use of chemicals causes soil contamination and nutritional stress. *Intechopen*.eds: Larramendy ML,Soloneski S.
44. Peiris C, Gunatilake S.R, Wewalwela J.J, Vithanage M., (2019). Biochar for sustainable agriculture: Nutrient dynamics, soil enzymes, and crop growth. In *Biochar from biomass and waste Elsevier* 211–224.
45. Phairuang W,SuwattigaP,ChetianukornkulT, Hongtieab S,Limpaseni W,IkemoriF, HataM, FuruuchiM., (2019). The influence of the open burning of agricultural biomass and forest fires in Thailand on the carbonaceous components in size fractionated particles. *Environmental Pollution* 247:238-247.
46. Pal, S., Tak, Y.K., Song, J.M., (2007). Does the antibacterial activity of silver nanoparticles depend on the shape of the nanoparticle? A study of the gram-negative bacterium *Escherichia coli*. *Appl. Environ. Microbiol.* 73 (6), 1712–1720.
47. Pan, B.C., Han, F.C., Nie, G.Z., Wu, B., He, K., Lu, L., (2014a). New strategy to enhance phosphate removal from water by hydrous manganese oxide. *Environ. Sci. Technol.* 48 (9), 5101–5107.
48. Pan, B., Lin, D., Mashayekhi, H., Xing, B., (2008). Adsorption and hysteresis of Bisphenol A and 17 α -ethinyl estradiol on carbon nanomaterials. *Environ. Sci. Technol.* 42 (15), 5480–5485.
49. Pan, B.J., Qiu, H., Pan, B.C., Nie, G.Z., Xiao, L.L., Lv, L., Zhang,W.M., Zhang, Q.X., Zheng, S.R., (2010). Highly efficient removal of heavy metals by polymer-supported nanosized hydrated Fe(III) oxides: behavior and XPS study. *Water Res.* 44 (3), 815–824.
50. Pan, B.C., Wan, S.L., Zhang, S.J., Guo, Q.W., Xu, Z.C., Lv, L., Zhang, W.M., (2014b). Recyclable polymer-based nano-hydrous manganese dioxide for highly efficient Tl(I) removal from water. *Sci. China Chem.* 57 (5), 763–771.
51. Pan, B.J., Wu, J., Pan, B.C., Lv, L., Zhang, W.M., Xiao, L.L., Wang, X.S., Tao, X.C., Zheng, S.R., (2009). Development of polymer-based nanosized hydrated ferric oxides (HFOs) for enhanced phosphate removal from waste effluents. *Water Res.* 43 (17), 4421–4429.
52. Pan, B.C., Xu, J.S.,Wu, B., Li, Z.G., Liu, X.T., (2013). Enhanced removal of fluoride by polystyrene anion exchanger supported hydrous zirconium oxide nanoparticles. *Environ. Sci.Technol.* 47 (16), 9347–9354.
53. Piper C.S.,1966.*Soil plant analysis*. Hans Publishers, Bombay, India.
54. PradhanS,MackeyH.R,Al-AnsariT.A, McKay G., (2022). Biochar from food waste: a sustainable amendment to reduce water stress and improve the growth of chickpea plants. *Biomass Conversion and Biorefinery*12:4549-4562.
55. Rajkovich S, Enders A, Hanley K, Hyland C, Zimmerman AR, Lehmann J.,(2012). Corn growth and nitrogen nutrition after additions of biochars with varying properties to a temperate soil. *Biol. Fertil. Soils* 48: 271-284.
56. Sajanlal, P.R., Pradeep, T., 2008. Electric-field-assisted growth of highly uniform and oriented gold nanotriangles on conducting glass substrates. *Adv. Mater.* 20 (5), 980.
57. Schmid, G., (1992). Large clusters and colloids - metals in the embryonic state. *Chem. Rev.* 92 (8), 1709–1727.
58. Scocchi, G., Posocco, P., Fermeglia, M., Pricl, S., 2007. Polymer-clay nanocomposites: a multiscale molecular modeling approach. *J. Phys. Chem. B* 111 (9), 2143–2151.
59. Schimmelpfennig S, Glaser B., (2012). One step forward toward characterization: some important material properties to distinguish biochars. *J Environ Qual* 41:1001–1013.
60. Shabani, A.M.H., Dadfarnia, S., Dehghani, Z., (2009). On-line solid phase extraction system sing 1, 10-phenanthroline immobilized on surfactant coated alumina for the flame atomic absorption spectrometric determination of copper and cadmium. *Talanta* 79 (4), 1066–1070.
61. Shan, C., Ma, Z.Y., Tong, M.P., Ni, J.R., (2015). Removal of Hg(II) by poly(1-vinylimidazole)- grafted Fe₃O₄@SiO₂ magnetic nanoparticles. *Water Res.* 69, 252–260.
62. Shao, D.D., Hu, J., Jiang, Z.Q., Wang, X.K., (2011). Removal of 4,4'-dichlorinated biphenyl from aqueous solution using methyl methacrylate grafted multiwalled carbon nanotubes. *Chemosphere* 82 (5), 751–758.
63. Soares J.C, SantosC.S, Carvalho S.M.P, PintadoM.M, VasconcelosM.W., (2019). Preserving the nutritional quality of crop plants under a changing climate: importance and strategies. *Plant and Soil* 443:1-26.

64. Soil Science - An Introduction, (2015). Indian Society of Soil Science, ICAR Publications, New Delhi, India.
65. Stanford S, English L., (1949). Use of flame photometer in rapid soil tests of K and Ca. *Agron. J* 41:446-447.
66. Subbiah BV, Asija C.L., (1956). A rapid procedure for the estimation of available nitrogen in soils. *Curr. Sci* 25: 259-260.
67. Sumner M.E, Miller W.P., (1996). Cation exchange capacity and exchange coefficients. In: Sparks DL, Page AL, Helmke PA, Loepfert RH, Soltanpour PN, Tabatabai MA, Johnston CT, Sumner ME (eds), *Methods of Soil Analysis, Part 3. Chemical Methods*. American Society of Agronomy and Soil Science Society of America, Madison, Wisconsin, pp.1201-1229.
68. Tang J, Xi T., (2008). Status of biological evaluation on silver nanoparticles. *J. Biomed. Eng.* 25 (4), 4.
69. Tang, J.L., Xiong, L., Wang, S., Wang, J.Y., Liu, L., Li, J.A., Wan, Z.Y., Xi, T.F., (2008). Influence of silver nanoparticles on neurons and blood-brain barrier via subcutaneous injection in rats. *Appl. Surf. Sci.* 255 (2), 502-504.
70. Tang, J.L., Xiong, L., Wang, S., Wang, J.Y., Liu, L., Li, J.G., Yuan, F.Q., Xi, T.F., (2009). Distribution, translocation and accumulation of silver nanoparticles in rats. *J. Nanosci. Nanotechnol.* 9 (8), 4924-4932.
71. Tang, J.L., Wang, S., Liu, L., Wang, C.R., Xi, T.F., (2013). A preliminary study on the dose-effect relation when silver nanoparticles crossing through the blood-brain barrier in vitro. *Chinese J. Inorg. Chem.* 29 (5), 1025-1030.
72. Verheijen F, Jeffery S, Bastos A., (2010). Biochar application to soils- a critical scientific review of effects on soil properties, processes and functions. European Commission, Report EUR 24099EN, Luxembourg.
73. Walkley A, Black C.A., 1934. An examination of the wet acid methods for determining soil organic matters and proposed modification of the chromic acid titration method. *J. Soil Sci.*, 37: 29-38.
74. Wang L, OkY.S, Tsang D.C.W, Alessi DS, Rinklebe J, Masek O, Bolen N.S, Hou D., (2021). Biochar composites: Emerging trends, field successes and sustainability implications. *Soil Use & Management*.
75. Wang, X., Cai, W., Lin, Y., Wang, G., Liang, C., 2010a. Mass production of micro/nanostructured porous ZnO plates and their strong structurally enhanced and selective adsorption performance for environmental remediation. *J. Mater. Chem.* 20 (39), 8582.
76. Wang, Z., Yu, X., Pan, B., Xing, B., (2010b). Norfloxacin sorption and its thermodynamics on surface-modified carbon nanotubes. *Environ. Sci. Technol.* 44 (3), 978-984.
77. Wang, H., Yuan, X.Z., Wu, Y., Huang, H.J., Zeng, G.M., Liu, Y., Wang, X.L., Lin, N.B., Qi, Y., (2013). Adsorption characteristics and behaviors of graphene oxide for Zn(II) removal from aqueous solution. *Appl. Surf. Sci.* 279, 432-440.
78. Wang, J., Zhang, S.J., Pan, B.C., Zhang, W.M., Lv, L., (2011). Hydrous ferric oxide-resin nanocomposites of tunable structure for arsenite removal: effect of the host pore structure. *J. Hazard. Mater.* 198, 241-246.
79. Wislocki, G.B., Ladman, A.J., (1955). The demonstration of a blood-ocular barrier in the albino rat by means of the intravitam deposition of silver. *J. Biophys. Biochem. Cytol.* 1(6), 501-510.
80. Wu, M.C., Ma, B.H., Pan, T.Z., Chen, S.S., Sun, J.Q., (2016). Silver-nanoparticle-colored cotton fabrics with tunable colors and durable antibacterial and self-healing super hydrophobic properties. *Adv. Funct. Mater.* 26 (4), 569-576.

CITATION OF THIS ARTICLE

Mathesh A, Arivazhagan K, Senthilvalavan P, Natarajan S and Mathivanan N. Valorization of tapioca stem waste: Fabrication, characterization of biochar and iron enriched biochar and scheming of DTPA iron in acidic sandy loam soil. *Bull. Env. Pharmacol. Life Sci.*, Vol 12 [4] March 2023: 140-154